Analytical Methods

Accepted Manuscript

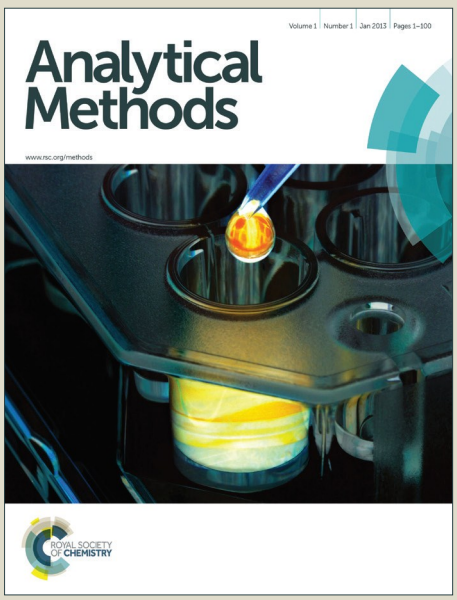

This is an *Accepted Manuscript*, which has been through the Royal Society of Chemistry peer review process and has been accepted for publication.

Accepted Manuscripts are published online shortly after acceptance, before technical editing, formatting and proof reading. Using this free service, authors can make their results available to the community, in citable form, before we publish the edited article. We will replace this *Accepted Manuscript* with the edited and formatted *Advance Article* as soon as it is available.

You can find more information about *Accepted Manuscripts* in the Information for Authors.

ROYAL SOCIETY OF CHEMISTRY

www.rsc.org/methods

Reagentless electrochemical immunosensor based on probes immobilization and layer-by-layer assembly technique for sensitive detection of tumor markers

Cong Qiumei,[a], Bian Hongmei,*[a], Yu Zhaoxia,[a] Jiyang Liu[b] and Fengna Xi*[b]

[a] *Oncology Department, Wendeng Central Hospital, Wendeng, Shandong Province, 264400, PR China*

[b]*Department of Chemistry, Zhejiang Sci-Tech University, Hangzhou, 310018, PR China*

Submitted to ***Analytical Methods***, Sep. 18, 2015

* Corresponding author. E-mail: Hongmeibian@126.com, Fengnaxi@zstu.edu.cn

Abstract

Facile electrochemical methods for highly sensitive detection of tumor markers provide great advances in early clinical diagnosis of cancer and public health protection. Herein, a reagentless electrochemical immunosensing platform was developed for sensitive immunoassay of the tumor biomarker based on surface-confined probes and layer-by-layer assembly technique. Ferrocene grafted cationic polymer polyethyleneimine (PEI-Fc) was modified on chemically reduced graphene oxide (rGO) to form redox-active and positively charged PEI-Fc-G nanocomposite. Through layer-by-layer electrostatic assembly technique, the positively charged PEI-Fc-G and negatively charged anionic polyelectrolyte poly(sodium-p-styrene-sulfonate) (PSS) were alternately assembled on negatively charged Au electrode. Based on biospecifIc binding of lectin and sugarprotein, *concanavalin A* (Con A) lectin monolayer served as the linker to immobilize sugarprotein (horseradish peroxidase, HRP) labeled anti-CEA antibody (HRP-Ab) on the surface of the $(PEI\text{-}Fc\text{-}G/PSS)_n$/PEI multilayer substrate. With carcinoembryonic antigen (CEA) being the model tumor biomarker, the as-prepared immunosensor presented high selectivity and good stability for sensitive and reagentless detection of CEA with a wide range of 0.1 ng/mL to 120 ng/mL (R^2 = 0.9963) and a detection limit as low as 60 pg/mL at a signal/noise ratio of 3. The proposed immunosensor might serve as a versatile platform for reliable cancer diagnostics clinical and biochemical analysis.

1. Introduction

Nowadays, cancer is considered as one of the most threatening diseases for human beings. Sensitive detection of tumor biomarkers plays an important role in disease prediction, early diagnosis and monitoring.[1,2] Based on specific antibody-antigen recognition, immunosensors such as chemiluminescence immunoassay and enzyme-linked immunoadsorbent assay have been developed for the detection of tumor biomarkers.[3,4] Recently, electrochemical immunosensors are one of the most widely used protocols in clinical and biochemical analysis due to the procedural simplicity, intrinsic sensitivity and low cost.[5-7] Generally, in the process of detection, most electrochemical immunosensors require introducing external chemicals into the electrolyte solution for generating electrochemical signals.[8-10] However, the introduction of solution-phase electrochemical indicators might compromise the detection performance due to the diffusion limit and contaminating of the target bio-systems. Now, increasing interests have been focused on reagentless electrochemical sensing platforms based on surface-confined signal indicators. Therefore, exploring new protocols and strategies to develop simple immunoassay systems for sensitive and reagentless detection of tumor biomarkers is of great significance. Effective immobilization of specific antibody on biocompatible redox-active matrix via simple procedures remains challenge and is highly desirable.

Functional electrode architecture plays critical roles in immunosensing performance. Nanomaterials are usually applied to achieve efficient detection in electrochemical bioanalysis. Graphene, as a rising star nanomaterial, has recently attracted tremendous interests in development of novel electrochemical biosensors because of its extraordinary electronic, chemical, structural, and mechanical properties.[11-14] However, graphene nanosheets tend to form agglomerates through

π-π stacking interactions. Since most unique properties of graphene are associated with individual nanosheets, the prevention of aggregation is important for the application of graphene. Aggregation can be reduced or overcome by covalent or non-covalent attachment of other molecules onto the surface of graphene sheets.[15-17] Through simple non-covalent interaction, graphene-polymer nanocomposites usually form homogeneous aqueous colloid solutions with individual nanosheets. Cationic polymers including polyethyleneimine (PEI), poly(diallyldimethylammonium chloride) (PDDA), poly(allylamine hydrochloride) (PAH) and chitosan have been used to prepared graphene-polymer nanocomposites.[13] It is supposed that redox-active graphene-polymer nanocomposites are ideal for fabricating highly sensitive and reagentless electrochemical immunosensors owing to its combination of the excellent conductivity of graphene and the redox activity of the modified electrochemical probes. For example, the modification of graphene sheets with Fc-grafted cationic polyelectrolyte would impart graphene with electrochemical redox activity, positively charged surface and good aqueous dispersity. Thus, the charged and redox active graphene-polyelectrolyte composite could be immobilized on electrode surface with a large amount by layer-by-layer (LBL) electrostatic assembly method, leading to a high current signal intensity and sensitivity. It is worth noting that both PEI and PAH are cationic polyelectrolyte and have primary amino groups (-NH2) to be used for covalent cross-linking with ferrocenecarboxaldehyde (Fc-CHO) through forming Schiff base. However, PEI possesses a much lower cost than that of PAH. Considering the low cost for constructing the immunosensor, we selected PEI as the initial material to synthesize Fc-grafted PEI (PEI-Fc) and PEI-Fc modified graphene (PEI-Fc-G) in this work.

Efficient immobilization of antibody without decreasing its binding affinity and capacities is

also important for fabricating high performance immunosensors. Nowadays, LBL assembly technique has been recognized as the ideal methodology for the immobilization of biomolecules due to its simplicity, versatility and biocompatible operation environment.[18] Despite electrostatic interaction usually used for LBL assembly, strongly biospecific affinity between lectin (e.g. *concanavalin A*, Con A), and sugar residues of sugarproteins (e.g. horseradish peroxidase, HRP) could be used. Using net charges of lectin at given pH, Con A self-assembled monolayer (SAM) could be achieved through electrostatic interaction.[19] The Con A SAM can provide an appropriate biomimetic interface for specific adhesion of sugarprotein, or sugarprotein-linked biomolecules. Therefore, sugarprotein labeled antibody (e.g. HRP labeled antibody) could be captured to demonstrate recognition interface for the immunoassay of the corresponding antigen. Compared with directly covalent immobilization of antibody, such indirect immobilization intermediated by lectin-sugarprotein interaction could enable the antibody to retain its binding affinity and capacity for target antigen.[20]

In this work, a sensitive and reagentless electrochemical immunosensing platform was constructed for immunoassay of the model tumor biomarker carcinoembryonic antigen (CEA) based on redox-active grapehene nanocomposites, LBL assembly technique and lectin-sugarprotein intermediated antibody immobilization. The redox-active graphene nanocomposite was prepared through non-covalent modification of chemically reduced graphene oxide (rGO) by Fc-grafted cationic polyelectrolyte PEI (PEI-Fc) and presented good electrochemical redox activity. LBL assembled graphene multilayer films were then fabricated on 3-mercaptopropionic acid (MPA) modified gold electrode surface for the immobilization of Con A SAM (Scheme 1). Based on biospecific binding of Con A and sugurprotein, HRP labeled anti-CEA

antibody (HRP-Ab) was captured on Con A SAM to form CEA recognition interface. Reagentless detection of CEA was demonstrated by using fast and sensitive differential pulse voltammetry (DPV) with surface-confined Fc molecules as signal indicators. The preparation methodology and main characteristic features of the immunosensor were described and discussed in detail.

2. Experimental

2.1. Reagents

Con A from *canavalia ensiformis* (Jack Bean), bovine serum albumin (BSA), and poly(ethylene imine) (PEI) were purchased from Sigma-Aldrich. Ferrocene-carboxaldehyde (98%) was purchased from J&K Chemical Ltd. CEA, HRP labeled anti-CEA antibody (HRP-Ab) and prostate specific antigen (PSA) were obtained from Keyuezhongkai Biotech Co., Ltd. (Beijing, China) and were stored at 4 °C before use. Poly(sodium-p-styrene-sulfonate) (PSS, MW 70 000) and 3-mercapto-1-propanesulfonic acid (MPA) were obtained from Aldrich. HRP (E.C.1.11.1.7, 250 U/mg) was purchased from Shanghai Sanjie Biotechnology Co., Ltd (Shanghai, China). All other chemicals were of analytical grade and used without further purification. Milli-Q water was used throughout the work. The real sample was obtained from Wendeng Central Hospital.

2.2. Apparatus and measurements.

Atomic force microscopy (AFM) was conducted on a SPI3800N microscope (Seiko Instruments, Inc.). Zeta potential measurements were performed on a Zetasizer Nano-ZS particle analyzer (Malvern, UK). Electrochemical measurements were performed on a CHI 660D electrochemical analyzer (Shanghai CH Instrument Company, China) at room temperature. A conventional three-electrode system was used with a bare Au electrode or modified Au electrode as the working

electrode, an Ag/AgCl electrode (saturated with KCl) as the reference electrode, and a platinum disk electrode as the auxiliary electrode, respectively. Cyclic voltammograms (CV) were measured in 0.1 M phosphate buffered solution (PBS, pH 7.4) by the potential scanning between 0.1 and 0.6 V. Differential pulse voltammetry (DPV) was carried out in 0.1 M PBS (pH 7.4) with the parameters as follows: modulation time 50 ms, interval time 0.5s, modulation amplitude 25 mV, step potential 5 mV, and voltage range from 0.1 to 0.6 V.

2.3. Preparation of PEI-Fc and PEI-Fc-G nanocomposites

PEI-Fc was firstly prepared by covalent cross-linking (forming Schiff base) between amine group of PEI and ferrocenecarboxaldehyde (Fc-CHO).[8] Briefly, PEI (0.6 g) was dissolved in 15 ml of methanol. Fc-CHO (80 mg) was dissolved in 10 ml of methanol. After PEI solution was added to a round-bottom flask (100 ml), 2 ml of triethylamine was added. Then, Fc-CHO solution was added with stirring for 2 h before sodium borohydride ($NaBH_4$, 18 mg) was added. A brown liquid was finally obtained. After methanol was evaporated at 50 °C, 3 ml Milli-Q water was added to dissolve the precipitate. The obtained product was placed in the dialysis membrane (6000-8000) for one-week dialysis. The obtained solution was collected and freeze-dried to obtain PEI-Fc.

PEI-Fc-G nanocomposites were prepared by wrapping PEI-Fc on rGO via non-covalent interaction. GO was prepared from natural graphite according to a modified Hummers' method.[9] For chemical reduction, GO dispersion (4.5 ml, 2 mg/mL) was mixed with 25.5 ml Milli-Q water. After the solution was added in a glass vial (100 ml), 13 μl of hydrazine solution (50% in water) and 100 μl of concentrated ammonia solution (28% in water) were added. After being vigorously shaken, the GO nanosheets were reduced to rGO nanosheets by refluxing the mixture at 75 °C for 3 h. After removing the large precipitate by centrifugation at 3000 rpm, then the stable rGO

dispersion was obtained. PEI-Fc-G nanocomposites were fabricated as follows. PEI-Fc (5 ml, 50 mg/mL) was added into the as-prepared rGO solution (20 ml). The obtained mixture was treated with ultrasonication (20 min) to form a uniform black dispersion. The resulting PEI-Fc-G nanocomposites were collected by centrifugation (15000 rpm) and washed with Milli-Q water for three times to remove free PEI-Fc. The resultant PEI-Fc-G nanocomposites were re-dispersed in Milli-Q water for further use.

2.4. Fabrication of the immunosensing interface

Au electrodes were used as the base electrodes. Before modification, a bare Au electrode was successively polished with emery paper and 0.05 μm α-Al_2O_3 slurry. After being ultrasonicated in Milli-Q water for 5 min, the electrode was immersed in a freshly prepared Piranha solution (30% H_2O_2 and concentrated H_2SO_4, 1:3 v/v) for 10 min. After being ultrasonicated in Milli-Q water, the electrode was electrochemically pretreated in 0.1 M H_2SO_4 by cyclic potential scanning between 1.4 and -0.2 V at a scan rate of 0.5 V/s until a standard cyclic voltammogram of clean Au electrode was obtained. After being washed thoroughly with water and dried in a nitrogen stream, the obtained clean Au electrode was immersed into a 0.1 M MPA ethanol solution for 10 h to assemble a negatively charged MPA monolayer on Au electrode through Au-S bounding interaction.

The fabrication process of the immunosensing interface was shown in Scheme 1 and three steps were involved. Firstly, $(PEI\text{-}Fc\text{-}G/PSS)_n$ multilayer film was prepared on Au/MPA based on electrostatic assembly of PEI-Fc-G nanocomposite and anionic polyelectrolyte PSS. The PSS solution (1 mg/mL) was prepared in barbital buffer (10 mM, pH 7.4). Au/MPA electrode was alternately dipped into the PEI-Fc-G aqueous solution (1 mg/mL, 40 min) and PSS solution (1

mg/mL, 20 min) to form (PEI-Fc-G/PSS)$_5$ multilayer on the Au/MPA electrode. Then the resultant electrode was immersed into a PEI solution (1 mg/mL) for 20 min to form Au/MPA/(PEI-Fc-G/PSS)$_5$PEI electrode with a positively charged surface on the outermost layer. Secondly, Con A SAM was immobilized on the as-prepared electrode by electrostatic interaction. The Au/MPA/(PEI-Fc-G/PSS)$_5$PEI electrode was dipped into a Con A solution (0.3 mg/ml) for 40 min and then washed with Milli-Q water. The Con A solution was prepared in barbital buffer (10 mM, pH 7.4) containing 1 mM $CaCl_2$ and 1 mM $MnCl_2$. Because Con A (p*I* 5.0) has negatively net charges at neutral pH,[19] it is able to form SAM on the electrode surface through electrostatic interaction between Con A molecules and positively charged PEI polyelectrolyte. The obtained electrode was denoted as Au/MPA/(PEI-Fc-G/PSS)$_5$PEI/Con A. Thirdly, HRP-Ab was specifically captured on the Con A SAM to demonstrate CEA recognition interface based on high affinity of Con A with saccharides existed in HRP. The Au/MPA/(PEI-Fc-G/PSS)$_5$PEI/Con A electrode was immersed in an HRP-Ab solution (100 μg/ml) for 1h. One Con A molecule has four binding sites of saccharide group. In order to reduce the nonspecific adsorption of CEA, the obtained electrode was finally incubated in an HRP solution (1 mg/ml) for 1h to block possible remaining free sites of Con A and the substrate film. The obtained immunosensor, Au/MPA/(PEI-Fc-G/PSS)$_5$/PEI/Con A/HRP-Ab electrode, was stored at 4 °C when not in use.

Scheme 1 near here

3. Results and discussion

3.1. Characterizations of rGO and PEI-Fc-G

AFM was used to characterize the surface morphology and thickness of the bare and polymer PEI-Fc modified rGO sheets. Fig. 1A and 1B show typical AFM images of rGO and PEI-Fc-G

nanosheets on freshly cleaved mica. Fig. 1C and 1D display the corresponding cross-sectional views of rGO and PEI-Fc-G, respectively. As seen from Fig 1A, the rGO sheets are well separated and ultra-thin paper like single sheet with an extremely smooth surface. Measured from the height profile of the AFM image (Fig 1C), the average thickness of rGO is 0.83 nm, which is nearly consistent with literature data.[21] After functionalizing rGO with PEI-Fc, the resulted PEI-Fc-G composite shows a rough surface structure (Fig 1B) and has an average thickness of about 4.2 nm (Fig 1D). The greater thickness of PEI-Fc-G than that of rGO indicated that the polymer PEI-Fc molecules were successfully attached onto both sides of rGO sheets with a large quantity. The zeta potentials of rGO and PEI-Fc-G in aqueous solution were measured to be -36.2 mV and +38.8 mV, respectively. The PEI-Fc-G could disperse well and possessed a good stability in aqueous solution. This is mainly ascribed that the modified cationic polyelectrolyte PEI effectively obstructs the π-π stacking interaction between graphene sheets and imparts graphene surface with a large amount of positive charge, leading to a strong electrostatic interaction between PEI-Fc-G sheets. Thus, the positively charged PEI-Fc-G composite with good aqueous dispersity shows potential as a cationic block for LBL electrostatic self-assembly. Combined with its redox activity, this composite might be of particular interest for the construction of reagentless electrochemical sensing platforms.

Fig. 1 near here

3.2. Electrochemical Characterization of graphene multilayer-modified electrode

The process of the PEI-Fc-G/PSS multilayer film assembling on the MPA modified Au electrode was characterized by cyclic voltammetry. As shown in Fig 2A, the cyclic voltammograms (CVs) of the modified Au electrode assembled with different number of PEI-Fc-G/PSS bilayer shows a

pair of well defined redox peaks located at 0.422 and 0.375 V, which represent the oxidation and reduction of the surface-confined Fc molecules.[8] With increasing the number of PEI-Fc-G/PSS bilayer from 1 to 5, the redox peak currents increase linearly, suggesting that the assembling process could be well controlled (inset of Fig. 2A). According to the standards below, we fixed the final PEI-Fc-G/PSS bilayer number at five, resulting in the Au/MPA/(PEI-Fc-G/PSS)5 modified electrode. Firstly, the electrochemical signal originated from the immobilized probes should provide both appropriate intensity and high sensitivity for the immunosensor. Secondly, when the thickness of the multilayer film reached a certain value, it would not effectively promote the electron transfer of the immobilized electrochemical probes. Thirdly, once the signal intensity and sensitivity were guaranteed, the fabrication of the immunosensor should be more simple and convenient. While considering time consuming and low cost, we fixed the PEI-Fc-G/PSS bilayer number at five even the bilayer number higher than five could provide higher current response. It is noted that the CV peak current density of the $(PEI\text{-}Fc\text{-}G/PSS)_5$ multilayer modified Au electrode is measured to be 740 $\mu A/cm^2$, which is about 22 times higher than previously reported 33 $\mu A/cm^2$ of the $(PEI\text{-}Fc/CNTs)_5$ multilayer modified ITO electrode.[22] This result suggests that the direct modification of PEI-Fc on graphene to form an integrated composite could promote electron transfer of Fc with a higher efficiency. Thus, the electrode modified with $(PEI\text{-}Fc\text{-}G/PSS)_5$ multilayer could produce a high current signal intensity and be benefited to construct high sensitive electrochemical sensing platforms.

Fig. 2 near here

Fig. 2B shows the cyclic voltammograms (CVs) of the prepared Au/MPA/$(PEI\text{-}Fc\text{-}G/PSS)_5$ electrode at different scan rates. It can be seen that both the anodic and cathodic peak currents

linearly increase with increasing the scan rate from 40 to 300 mV/s (inset of Fig. 2B), suggesting a surface-controlled electrochemical process for the electron transfer between the surface-confined Fc molecules and substrate electrode. The peak-to-peak separation is nearly independent of the scan rate, indicating that graphene can effectively promote the electron transfer of Fc. Additionally, the current response of the modified electrode has no obvious change after continuous potential scan of 40 segments (both the anodic and cathodic peak currents decreased less than 1.2%), suggesting that the assembled multilayer film has a good electrochemical stability on the electrode surface.

3.3. Characterization of recognition interface on graphene multilayer

The fabrication and CEA detection of recognition interface were evaluated by cyclic voltammetry in 0.1 M PBS (pH 7.4). As shown in Fig. 3, the Au/MPA/(PEI-Fc-G/PSS)$_5$ electrode shows a large current signal of Fc (curve a). To improve the stability of Fc and immobilize the lection, (PEI-Fc-G/PSS)$_5$ multilayer was further assembled with a positively charged PEI. After binding with Con A, the obtained Au/MPA/(PEI-Fc-G/PSS)$_5$/PEI/Con A electrode has an obvious decrease in the peak currents response due to its insulativity of protein Con A (curve b). When HRP-Ab is assembled on the Con A modified electrode, the peak currents further decrease (curve c), suggesting an efficient immobilization of antibody. After blocking the Au/MPA/(PEI-Fc-G/PSS)$_5$/PEI/Con A/HRP-Ab electrode with HRP, the finally fabricated sensing interface also has a little reduction of the peak current response (curve d). By incubating the sensing electrode in 5 ng/mL CEA solution for 30 min, the CV peak currents continue to decrease (curve e), indicating that the immobilized anti-CEA antibodies on the interface can effectively recognize and capture CEA antigen, inducing a larger coverage on the electrode surface to inhibit

the electrochemical current signal of Fc probes.

Fig. 3 near here

3.4. Electrochemical Detection of CEA with the fabricated immunosensor

Differential pulse voltammetry (DPV) was used for electrochemical detection of CEA. In most reported electrochemical immunosensors, external chemicals such as $[Fe(CN)_6]^{3-/4-}$ redox probes were usually introduced into the electrolyte solution to generate electrochemical signals.[20] The reagentless detection in this investigation used surface-confined Fc as the signal indicator to detect CEA, which could avoid any possible contamination caused by external redox probes. The mechanism of electrochemical detection of CEA was described as following. The redox process of the surface-confined Fc includes two steps.[8,23] One step is the electron transfer between Fc and substrate electrode. The other step is the transfer of solvated anions between electrolyte solution and Fc. Once CEA was binding onto the sensing interface, the formed antigen-antibody complex would produce a larger coverage on the electrode surface and isolate the interface from the electrolyte solution, which would inhibit the transfer of solvated anions between the electrolyte solution and Fc, leading to a decrease in current response. The decrease of DPV peak current of the immunosensor is directly related to the amount of the captured CEA molecules. More CEA molecules binding on the electrode would produce a larger coverage and lead to a lower current response. This is the basic principle for the reagentless immunosenor to detect CEA.

Fig. 4 near here

One important factor influencing the CEA capture is the incubation time of immunosensor in the CEA solution. The kinetic experiment was carried out to determine the optimum incubation time for CEA detection. As shown in Fig. 4, the DPV peak current response of the immunosensor

decreases significantly with the increase of incubation time in 5.0 ng/ml of CEA solution and reached a plateau after incubation for 30 min. Thus, the optimum incubation time was selected as 30 min.

Fig. 5 near here

Fig. 5A shows the DPV responses of the immunosensor to CEA solutions at different concentrations. With increasing the concentration of CEA, the DPV anodic peak current decreases significantly, indicating a higher amount of CEA binding to the sensing interface. When the concentration of CEA is increased to 500 ng/ml, the DPV peak current no longer decreases, suggesting that the coverage of CEA on the sensing interface has reached a maximal limit. In Fig. 5B, the ratio of I/I_0 was used to evaluate the DPV anodic peak current responding to CEA solution at different concentration, where I and I_0 represent peak current response of the immunosensor before and after incubation in CEA solution at a certain concentration, respectively. As seen from the inset of Fig. 5B, there is a linear relationship between I/I_0 and logarithm of CEA concentration from 0.1 to 120 ng/ml. The corresponding linear regression equation is I/I0=(-0.2168±0.0035)log[CEA]+(0.7246±0.0066), R2 = 0.9963. The detection limit is evaluated as 60 pg/ml at a signal to noise ratio of 3, which is lower than that of those conventional electrochemical immunosensors using external redox probes as signal indicator, such as the systems based on AuNPs/CNT-CS (two linear range of 0.3-2.5 and 2.5-20 ng/mL with a detection limit of 0.01 ng/mL),[24] and the latest reported 3D graphene foam based three dimension (3D) immunosensor (linear range of 0.1-750.0 ng/mL with a detection limit of 90 pg/ml).[20] Moreover, it is lower than that of label-free immunosensors using carboxyl graphene nanosheets–methylene blue (CGS-MB) on indium-tin oxide (ITO) branched electrode system (linear range of

0.5-80.0 ng/mL with a detection limit of 0.05 ng/ml), [25] and the gold nanoparticles (AuNPs) decorated reduced graphene oxide (rGO)-carried Prussian blue (PB) system (linear range of 0.6-80.0 ng/mL with a detection limit of 0.12 ng/ml).[26] As well known, effective antibody immobilization is of importance for improving the detection performance of immunosensors. The good performance could be attributed to the antibody immobilization based on lectin-sugarprotein interaction, which offers an indirect and oriented immobilization on the matrix. Additionally, the combination of graphene hybrid redox probes and LBL assembly technique effectively improved its sensitivity of the fabricated immunosensor.

Fig. 6 near here

3.5. Selectivity, reproducibility and stability of the immunosensor

The specificity of the immunosensor was examined by testing the DPV response toward different interferences such as prostate specific antigen (PSA), bovine serum albumin (BSA), and horseradish peroxidase (HRP) solutions prepared in blank PBS (0.1 M, pH 7.4). The DPV current signals of the immunosensor incubated in the blank PBS, BSA (1 μg/mL), PSA (1 μg/mL), HRP (1 μg/mL) and CEA (5.0 ng/mL) were recorded and the comparison results were shown in Fig. 6. It can be seen that the DPV responses of the interferences including PSA (Fig. 6A), BSA (Fig. 6B), and HRP (Fig. 6C) are nearly the same as that of the blank PBS. However, there is a remarkable decrease in DPV peak current for the sample of CEA (5.0 ng/mL) in comparison with that of the blank PBS (Fig. 6D), indicating that the immunosensor presented good specificity towards the detection of CEA. To evaluate the reproducibility of the immunosensor, three electrodes were prepared to detect 5.0 ng/mL of CEA. The relative standard deviation (RSD) of the measurements was 3.7%, suggesting a good reproducibility of the proposed immunosensor. The stability of the

immunosensor was also examined over a 14-day period by detecting the current response to 5.0 ng/mL of CEA. When not in use, the immunosensor was stored at 4 °C. The DPV response maintained about 94.8% of the original value, indicating a good stability of the fabricated immunosensor.

3.6. Real sample analysis

To evaluate the analytical reliability and practical applicability of this immunosensor for real sample analysis, recovery experiments was performed using diluted human serum (1:9 diluted with 0.1 M PBS, pH 7.4) as the matrix.[3,27] Though human serum contains a large variety of biomolecules, no obvious change was observed after the immunosensor was incubated in it for 30 min. Different CEA (1.0, 2.0, 5.0 ng/mL) spiked serum samples were detected by DPV measurement. The results were shown in Table 1. The CEA recovery was between 95% and 103% and the RSD was less than 4.7% (n=3). The results definitely demonstrated the potential application of this immunosensor in real serum samples. Three positive serum specimens supplied by the Wendeng Central Hospital, PR China, were determined by both the proposed electrochemical immunosensor and the enzyme-linked immunosorbent assay (ELISA) methods, respectively. In a clinical setting, the sample was directly tested without dilution. If the results were very close to or exceeding the highest concentration of the calibration ranges, it had to be diluted using blank PBS (0.1 M PBS, pH 7.4) for further determination. The linear range for CEA determination in ELISA method was 5.0-80.0 ng/mL (ELISA kit for human CEA determination was supplied by Autobio diagnostics Co. Ltd, China). As demonstrated in Table 2, the CEA concentrations of the three un-diluted samples were all in the calibration ranges of both the electrochemical immuonosensor and the referenced ELISA method. In addition, there was no

significant difference between the results given by two methods. Therefore, the proposed sensor could be reasonably applied in the clinical determination of CEA in human serum.

4. Conclusion

Based on surface-confined probes fabricated with LBL assembly technique, a reagentless electrochemical immunosensor was simply fabricated to detect CEA. The PEI-Fc-G hybrid probes exhibited high electron transfer efficiency. Through LBL assembly method, a large amount of the hybrid redox probes were immobilized on the electrode with good controllability and stability. In addition, the effective antibody immobilization mediated by lectin-sugarprotein interaction offers an indirect and oriented immobilization on the substrate. Combined with these benefits, the fabricated sensor presented good performance in terms of wide detection range, high sensitivity, and low detection limit. Meanwhile, it also possessed good selectivity, reproducibility and stability. The proposed fabrication method could be used as a versatile way for constructing various reagentless immunosensor to detect other tumor makers and held promising potential for reliable cancer diagnostics in clinical and biochemical analysis.

Acknowledgements

The authors gratefully acknowledge the financial support from the National Natural Science Foundation of China (No. 21305127) and the Zhejiang Provincial Natural Science Foundation of China (Y15B050022).

References

1 A. J. Haque, H. J. Park, D. K. Sung, S. Y. Jon, S. Y. Choi and K. W. Kim, *Anal. Chem.*, 2012, **84**, 1871.

2 K. P. Liu, J. J. Zhang, C. M. Wang and J. J. Zhu, *Biosens. Bioelectron.*, 2011, **26**, 3627.

3 C. Leng, J. Wu, Q. N. Xu, G. S. Lai, H. X. Ju and F. Yan, *Biosens. Bioelectron.*, 2011, **27**, 71.

4 B. L. Su, D. P. Tang, J. Tang, Y. L. Cui and G. N. Chen, *Biosens. Bioelectron.*, 2011, **30**, 229.

5 Z. Q. Jiang, C. F. Zhao, L. Q. Lin, S. H. Weng, Q. C. Liu and X. H. Lin, *Anal. Methods*, 2015, **7**, 4508.

6 J. Tang, D. P. Tang, R. Niessner, G. N. Chen, D. Knopp, *Anal. Chem.*, 2011, **83**, 5407.

7 G. L. Yuan, J. L. He, Y. Li, W. L. Xu, L. L. Gao and C. Yu, *Anal. Methods*, 2015, **7**, 1745.

8 J. Y. Liu, Y. N. Qin, D. Li, T. S. Wang, Y. Q. Liu, J. Wang and E. K. Wang, *Biosens. Bioelectron.*, 2013, **41**, 436.

9 R. Li, D. Wu, H. Li, C. X. Xu, H. Wang, Y. F. Zhao, Y. Y. Cai, Q. Wei and B. Du, *Anal. Biochem.*, 2011, **414**, 196.

10 C. X. Li, X. Y. Qiu, K. Q. Deng and Z. H. Hou, *Anal. Methods*, 2014, **6**, 9078.

11 Y. W. Hu, K. K. Wang, Q. X. Zhang, F. H. Li, T. S. Wu and L. Niu, *Biomaterials*, 2012, **33**, 1097.

12 F. N. Xi, D. J. Zhao., X. W. Wang and P. Chen, *Electrochem. Commun.*, 2013, 26, 81.

13 Y. Liu, X. C. Dong and P. Chen, *Chem. Soc. Rev.*, 2012, **41**, 2283.

14 J. Y. Liu, X. H. Wang, T. S. Wang, D. Li, F. N. Xi, J. Wang and E. K. Wang, *ACS Appl. Mater. Interfaces*, 2014, **6**, 19997.

15 Y. Y. Xie, A. Q. Chen, D. Du and Y. H. Lin, *Anal. Chim. Acta*, 2011, **699**, 44.

16 Y. L. Yuan, X. X. Gou, R. Yuan, Y. Q. Chai, Y. Zhuo, X. Y. Ye and X. X. Gan, *Biosens. Bioelectron.*, 2011, **30**, 123.

17 J. Y. Liu, L. Han, T. S. Wang, W. Hong, Y. Q. Liu and E. K. Wang, *Chem. Asian J.*, 2012, **7**, 2824.

18 M. Matsusaki, H. Ajiro, T. Kida, T. Serizawa and M. Akashi, *Adv. Mater.*, 2012, **24**, 454.

19 F. N. Xi, J. Q. Gao, J. E. Wang and Z. X. Wang, J. *Electroanal. Chem.*, 2011, **656**, 252.

20 J. Y. Liu, J. Wang, T. S. Wang, D. Li, F. N. Xi, J. Wang and E. K. Wang, *Biosens. Bioelectron.*, 2015, **65**, 281.

21 D. Li, M. Muller, S. Gilje, R. Kaner and G. Wallace, *Nat. Nanotechnol.*, 2008, **3**, 101.

22 D. Yan, C. G. Chen, B. L. Li, M. Zhou, E. K. Wang and S. J. Dong, *Biosens. Bioelectron.*, 2010, **25**, 1902.

23 D. Han, Y. R. Kim, J. W. Oh, T. H. Kim, R. K. Mahajan, J. S. Kim and H. Kim, *Analyst*, 2009, **134**, 1857.

24 K. J. Huang, D. J. Niu, W. Z. Xie and W. Wang, *Anal. Chim. Acta*, 2010, **659**, 102.

25 F. Kong, B. Xu, Y. Du, J. Xu and H. Chen, *Chem. Commun., 2013,* **49***,* 1052.

26. D. Feng, L. Lia, X. Hana, X. Fenga, X. Lib and Y. Zhang, *Sensor. Actuat. B-Chem*., 2014, **201**, 360.

27. M. Emami, M. Shamsipur, R. Saber and R. Irajirad,, *Analyst*, 2014, **139**, 2858.

Figure Captions

Scheme 1 Schematic routine for the fabrication and CEA detection of the reagentless electrochemical immunosensor.

Fig. 1 Tapping mode AFM images of rGO (A) and PEI-Fc-G (B) on freshly cleaved mica.

Fig. 2 (A) CVs of Au/MPA/(PEI-Fc-G/PSS)$_n$ electrodes in PBS (0.1 M, pH 7.4) supporting electrolyte. The subscript n represents the number of PEI-Fc-G/PSS bilayer, n=1, 2, 3, 4, 5 (from inner to outer). Scan rate: 100 mV/s. Inset shows the linear relationship between peak currents and the number of bilayer. (B) CVs of the Au/MPA/(PEI-Fc-G/PSS)$_5$ electrode in PBS (0.1 M, pH 7.4) supporting electrolyte at different scan rates from 40 to 300 mV/s. Inset shows linear relationship between the peak current and scan rate.

Fig. 3 CVs of different modified electrodes recorded in 0.1 M PBS (pH 7.4) at a scan rate of 100 mV/s. (a) Au/MPA/(PEI-Fc-G/PSS)$_5$, (b) Au/MPA/(PEI-Fc-G/PSS)$_5$/PEI/Con A, (c) Au/MPA/(PEI-Fc-G/PSS)$_5$/PEI/Con A/HRP-Ab, (d) Au/MPA/(PEI-Fc-G/PSS)$_5$/PEI/Con A/HRP-Ab after blocked by HRP, and (e) Au/MPA/(PEI-Fc-G/PSS)$_5$/Con A/HRP-Ab incubated with 5.0 ng/mL CEA.

Fig. 4 The time-dependent DPV signal responses of the immunosensor for CEA detection in PBS (0.1 M, pH 7.4). I/I_0: I and I_0 represent peak current of the immunosensor before and after incubation in 5.0 ng/mLCEA solution. The error bars represent the relative standard deviation (RSD) of three measurements.

Fig. 5 (A) DPV responses of the immunosensor to CEA at different concentrations: 0, 0.1, 0.3, 1.0, 5.0, 20.0, 120.0, 500.0 ng/mL (from top to bottom). (B) The relative responses of the immunosensor to CEA at different concentrations (from 0 to 500.0 ng/mL). Inset shows the

calibration plot of I/I_0 versus logarithm of CEA concentration under optimal conditions. The error bars represent the RSD of three measurements.

Fig. 6 Selectivity evaluation of the immunosensor. CEA (5.0 ng/mL) shows an evident decrease in the DPV response (A). No obvious change of the DPV peak current for 1 μg/mL PSA (B), 1 μg/mL BSA (C), and 1 μg/mL HRP (D).

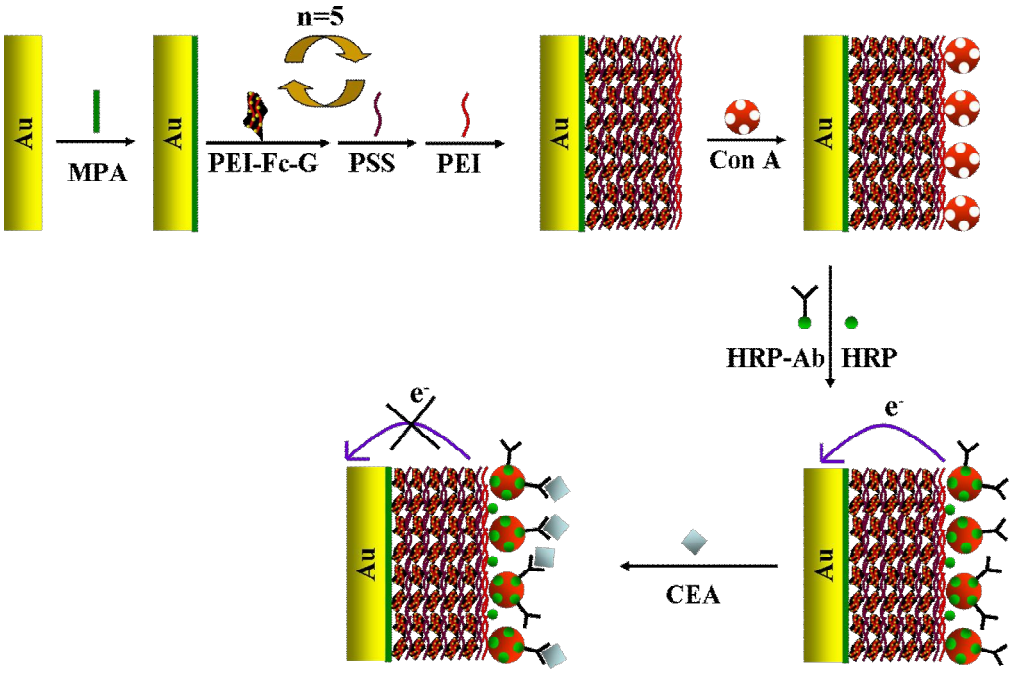

Scheme 1

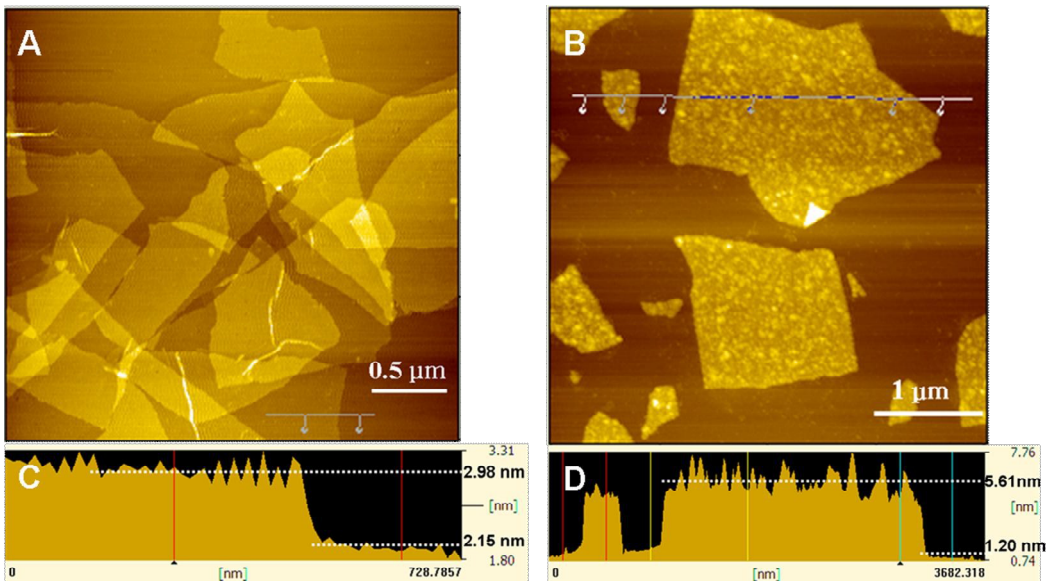

Fig. 1

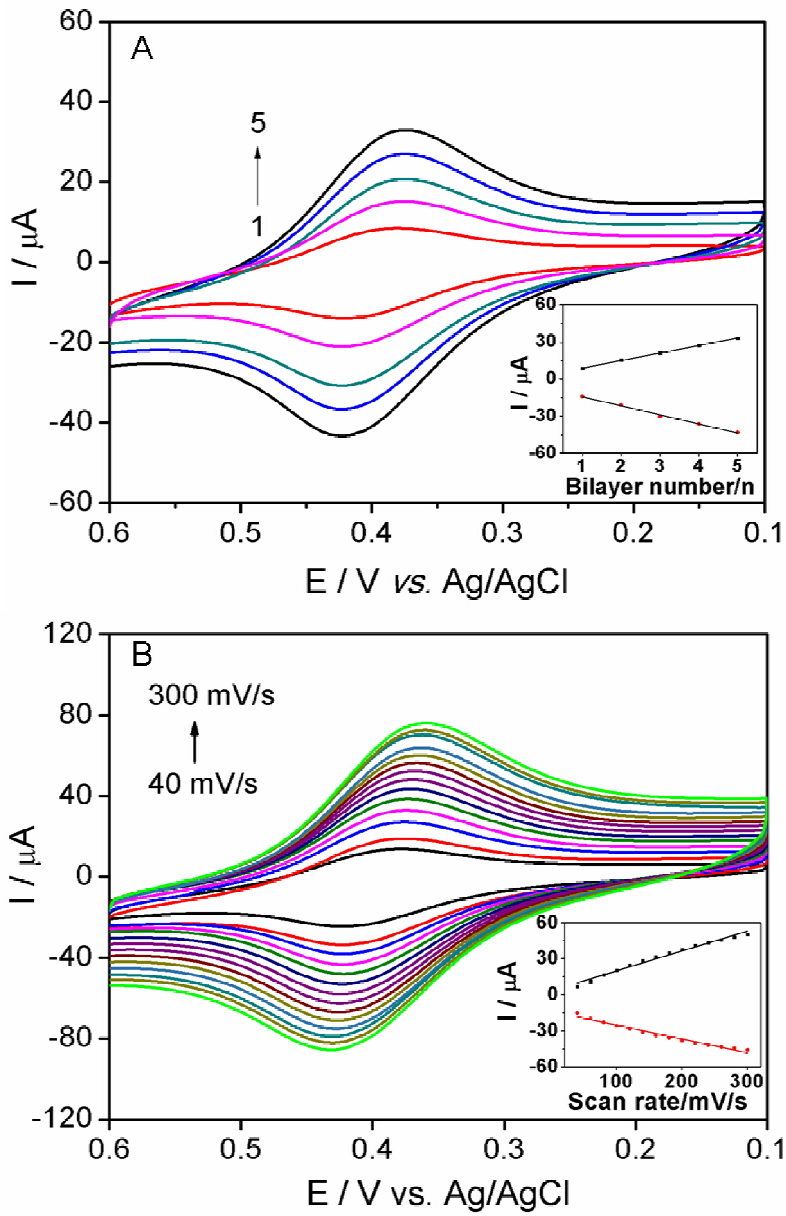

Fig. 2

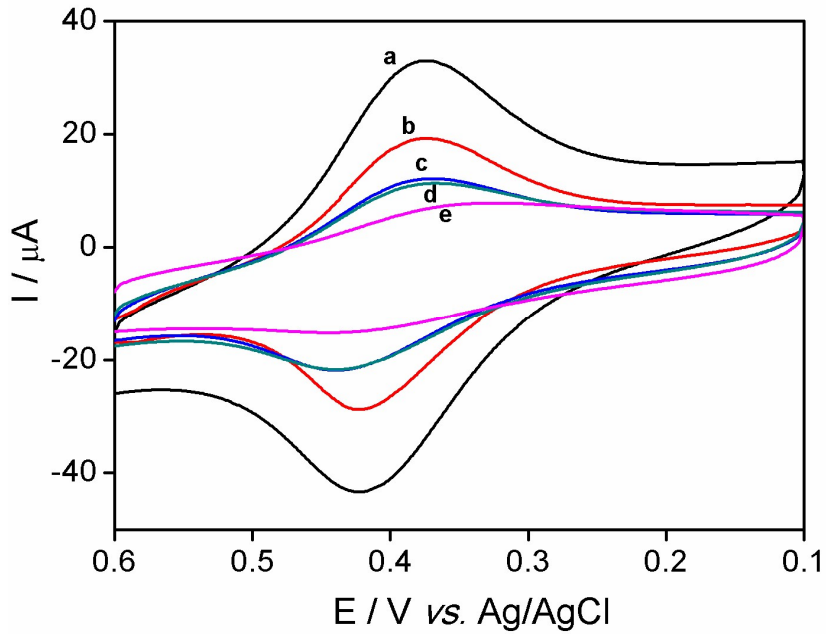

Fig. 3

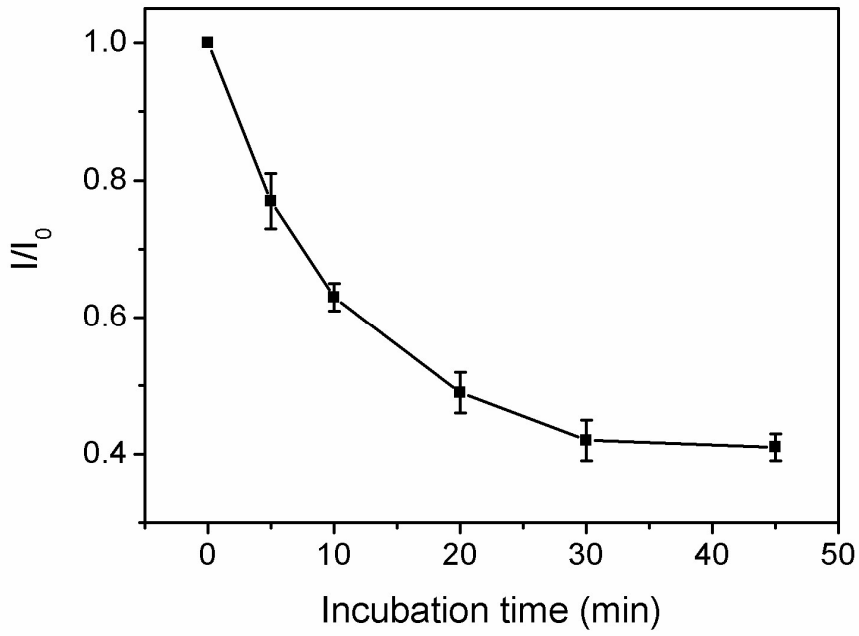

Fig. 4

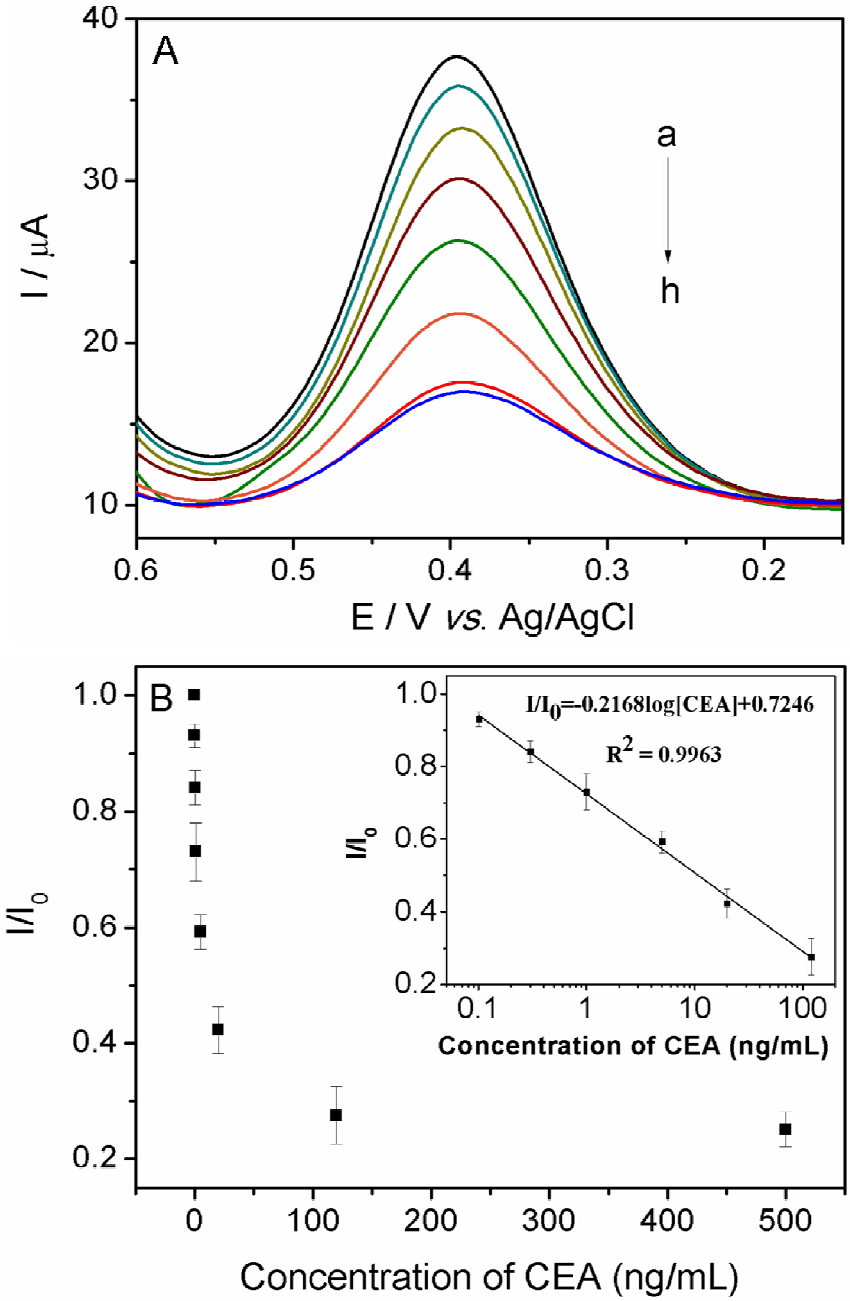

Fig. 5

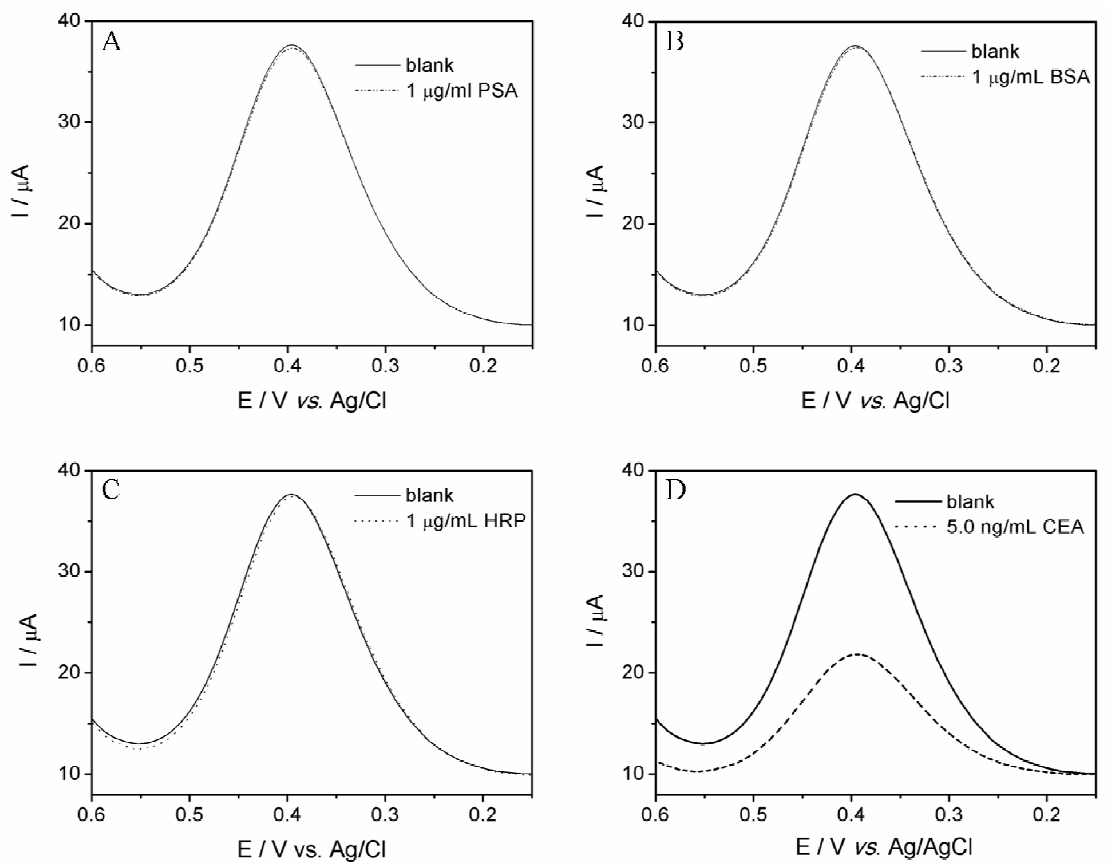

Fig. 6

Table 1

The result of CEA detection in diluted human serum by the immunosensor.

Diluted human serum (ng/ml)	The addition content (ng/ml)	The detection content (ng/ml)	RSD (%)	Recovery (%)
0	1.0	0.92, 1.01, 0.94	4.7	95.7
	2.0	2.07,1.99, 2.03	4.0	101.5
	5.0	5.13, 5.07, 5.16	4.6	102.4

Table 2

CEA detection by using the electrochemical immuonosensor and the referenced ELISA method.

Serum sample no.	Proposed method (ng/ml, n = 3)	ELISA method (ng/ml, n = 3)	Relative error (%)
1	29.0 ± 1.3	27.9 ± 1.1	3.9
2	15.6 ± 0.5	16.0 ± 0.6	2.5
3	9.8 ± 0.4	10.1 ± 0.3	3.0

Graphical abstract

Combined with surface-confined probes, lectin-sugarprotein interaction mediated antibody immobilization, and layer-by-layer assembly technique, a reagentless electrochemical immunosensor was constructed for highly sensitive detection of carcinoembryonic antigen.